Eco-Friendly Tri-Sodium Citrate as Corrosion Inhibitor for Mild Steel in Synthetic Cooling Water System

R. Touir[1,2,*], A. Koulou[1], M. Chahboune[1], Y. El Kacimi[1] and H. Larhzil[3]

[1]*Laboratory of Materials Engineering and Environment: Modeling and Application, Department of Chemistry, Faculty of Sciences, Ibn Tofail University, PO Box 133-14000, Kenitra, Morocco*

[2]*Regional Center of Education and Training Professions (CRMEF), 23 Street AbdelAziz Boutaleb, Mimousa, Kenitra, Morocco*

[3]*Laboratoire de Recherche Scientifique et Pédagogique dans le Monde Méditerranéen, Centre Régional des Métiers de l'Éducation et de la Formation, Meknès, Morocco*

Abstract: The influence of an ecofriendly tri-sodium citrate (TSC) on the inhibition of mild steel corrosion in synthetic cooling water was studied by using potentiodynamic polarization (PP), and electrochemical impedance spectroscopy (EIS) measurements. The state of mild steel surface was characterized by scanning microscopy electron (SEM) analysis. It is found that TSC acts as an anodic type inhibitor where its inhibition increases with concentration to reach a maximum of 89 % at 10^{-3} M. Indeed, the EIS plots revealed that TSC increases the polarization resistance of mild steel confirming the current-potential measurement and indicated that the inhibition efficiency of TSC increase with immersion time until 24 h of immersion. SEM investigation demonstrated that the inhibition of mild steel in corrosive/TSC solution was realized by the TSC molecules adsorption onto mild steel to prevent the dissolution process by blocking the active sites on its surface. Thus, it is shown that the TSC obey to the Langmuir isotherm and it is adsorbed via both physical and chemical adsorption which can explain by potential of zero charge (PZC) technique.

Keywords: Tri-sodium citrate; Corrosion inhibitor; Electrochemical measurements; Physical and chemical adsorption; SEM analysis.

1. INTRODUCTION

Iron and its alloy have been one of the most important and widely used materials in industrial application. They play a central role as basic material for cooling water systems. The corrosion and scale behavior of iron in are quite general and important phenomena cooling water systems. Thus, the corrosion problem has a great economic impact, since involves deterioration of a metallic surface. There is a great economic incentive in developing methods and materials to prevent this problem. There are several possibilities of protecting iron versus corrosion in severe media, where the practice of corrosion inhibitors is one the most economical and practical method.

It is generally assumed that organic compounds contain hetero-atoms such - S, - N, -O, -P atoms and/or aromatic rings or multiple bonds in their molecular structure have been reported to be good inhibitors [1-6]. Thus, there inhibition efficiency are mainly influenced by some their physicochemical and electronic properties which related to their functional groups and other factors [7, 8]. In addition, their effectiveness is usually attributed to their interactions with the metal surface via their adsorption, which depends on the metal surface charge, the inhibitor's chemical structure, and the nature of the electrolyte [9].

However, the use of corrosion inhibitors is increasingly being curtailed by recent environmental restrictions. So, in many parts of the world, high levels of organic and inorganic product are also restricted by law. Thus, inhibitors are diminishing, because of the concern over their toxic effects on aquatic and possibly animal life [10]. For this purpose, the use of green inhibitors is recommended. For example, gluconate sodium [11, 12], monosaccharide derivatives [13], citrate [14, 15] and phosphonate [16, 17], were used as eco-friendly corrosion inhibitors.

The goal of this study is to investigate the influence of tri-sodium citrate as environmental-friendly 'green' on the corrosion in cooling media under conditions similar to the typical operating conditions using electrochemical measurements and scanning electron microscopy analysis. Alternatively, the influence of immersion time and the mechanism action of TSC on mild steel were also studied and discussed.

2. EXPERIMENTAL PROCEDURE

2.1. Material, Inhibitor, Electrolyte and Electrochemical Cell

The used Pyrex electrolysis cell was closed by cap containing five openings where three of them were

*Address correspondence to this author at the Regional Center of education and training professions (CRMEF), 23 Street AbdelAziz Boutaleb, Mimousa, Kenitra, Morocco; Tel: +212 670 52 69 59; E-mail: touir8@yahoo.fr

ISSN: 1814-8085 / E-ISSN: 1927-5129/20

Table 1: Chemical Composition of Mild Steel in wt.%

C	Si	Mn	Cr	Mo	Ni	Al	Cu	Co	V	W	Fe
0.11	0.24	0.47	0.12	0.02	0.1	0.03	0.14	<0.0012	<0.003	0.06	Balance

Table 2: Composition of Synthetic Cooling Water

Salts	$MgCl_2$, $6H_2O$	$CaCl_2$,$2H_2O$	$Ca(NO_3)_2$,$6H_2O$	$MgSO_4$,$7H_2O$	$NaHCO_3$
Concentration (mg/L)	579.12	534.97	153.99	384.23	316.64
Conductivity (μS cm^{-1}) at 299 K	1678				

employed for the electrodes. The working electrode is mild steel with a surface area of 0.8 cm^2 and its chemical composition is exposed in Table **1**. Before each experiment, it electrode was polished using emery paper (until 1200 grade), cleaned with distillate water, degreased with ethanol, and finally dried with hot air. The rotating disk electrode used was an INF-EL-EDI 101 type. In addition, saturated calomel (SCE) and a platinum plate (S ≈ 2 cm^2) were used as a reference and auxiliary electrodes, respectively.

The used electrolyte is a synthetic cooling water solution where its composition is indicated in Table **2**. This composition represents the medium of the chemical elements presented in the real solution using in Moroccan cooling water system [11].

The organic compound tested is a tri-sodium citrate (TSC) which its molecular formula is shown in Figure **1**. So, this compound is commercial, non-toxic, easy handling, stable in air and inexpensive, used as a catalyst for an efficient for the synthesis of biological and pharmacological products [18], and in food industrial [19]. In addition, some research was focused to use tri-sodium citrate as an effective anticoagulation for continuous renal replacement therapy (CRRT) for patients with contraindications to heparin [20].

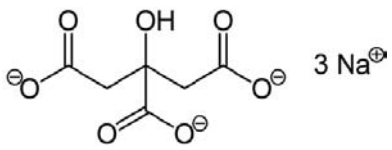

Figure 1: Molecular structure of tri-sodium citrate (TSC).

The temperature and pH were adjusted to 305 K and 7.3±0.02, respectively. The choice of this temperature is justified by the fact that it is the temperature of Moroccan cooling water circulation.

2.2. Electrochemical Measurements

The working electrode was immersed in the test medium during 1 h until a steady-state open circuit potential (E_{OCP}) was obtained. The disk rotation speed was 1000 rpm. The cathodic polarization curve was recorded by polarization from E_{OCP} to – 1000 mV/SCE with a sweep rate of 0.5 mV s^{-1}. After this scan, the anodic polarization curve was recorded by polarization from E_{ocp} to 200 mV/SCE with the same sweep rate. Since the conductivity of medium studied is low, the polarization curves i(E) were corrected from ohmic drop, where the solution resistance (R_s) was determined by electrochemical impedance spectroscopy.

The evaluation of kinetics parameters was determined using a fitting by Butler-Volmer equation (1). Thus, a nonlinear regression was made at the potential range limited to ± 0.050V around E_{corr}:

$$i = i_a + i_c = i_{corr}\left\{\exp\left[b_a \times \left(E - E_{corr}\right)\right] - \exp\left[b_c \times \left(E - E_{corr}\right)\right]\right\} \quad (1)$$

Where i_a , i_c , icorr, b_a and b_c are the anodic current, cathodic current, corrosion current density (A cm^{-2}), anodic and cathodic Tafel constants, respectively. These constants are linked to the Tafel slopes β (V/dec) in usual logarithmic scale given by equation (2):

$$\beta = \frac{\ln 10}{b} = \frac{2.303}{b} \quad (2)$$

The inhibition efficiency was calculated from the extracted i_{corr} values as follows:

$$\eta_{PP}\% = \frac{i_{corr}^0 - i_{corr}}{i_{corr}^0} \times 100 \quad (3)$$

where i^0_{corr} and i_{corr} are the corrosion current densities values without and with TSC, respectively.

The electrochemical impedance spectroscopy measurements were made with a small amplitude ac. signal (10 mV_{rms}), over a frequency domain from 100 kHz to 10 mHz. The results were then analyzed in terms of equivalent electrical circuit using Z-view program. The polarization resistance R_p, was obtained from the diameter of the semicircle in the Nyquist representation.

The inhibition efficiency (η_{EIS} %) and the surface coverage (θ) values were calculated as follows:

$$\eta_{EIS}\% = \frac{R_p - R_p^0}{R_p} \times 100 \quad (4)$$

$$\theta = \frac{R_p - R_p^0}{R_p} \quad (5)$$

where R^0_p and R_p are the polarization resistance values without and with TSC, respectively.

All electrochemical measurements were made using a Potentiostat/Galvanostat (VoltaLab PGZ 100) controlled by a personal computer.

2.3. Scanning Electron Microscopy (SEM)

The surface state of mild steel specimens in synthetic cooling water solution, without and with 10^{-3} M of TSC after 15 days immersion time, was carried out using scanning electron microscopy (SEM; JOEL JSM-5500).

3. RESULTS AND DISCUSSION

3.1. Electrochemical Measurement

The potentiodynamic polarization curves obtained for mild steel in synthetic cooling water solution without and with different concentration of TSC at 305 K are indicated in Figure **2** and their extracted parameters are illustrated in Table **3**.

Generally, it is assumed that the anodic reaction of iron in aerated neutral or basic solutions is the metallic iron (Fe) dissolution to ferrous cations (Fe^{2+}) as follows:

$$Fe \rightarrow Fe^{2+} + 2\,e^- \quad (6)$$

This iron oxidation process also issues electrons, which are inspired at the cathode through a reduction reaction as follows:

$$O_2 + 2\,H_2O + 4\,e^- \rightarrow 4\,HO^- \quad (7)$$

The above reactions (equation (6) and (7)) will produce corrosion products and HO^- ions causing the formation of iron hydroxides ($Fe(OH)_2$, $Fe(OH)_3$), oxides (Fe_3O_4, γ -Fe_2O_3), sulphates ($FeSO_4$) and chlorides ($FeCl_3$). Indeed, the presence of Ca(II) and HCO_3^- ions in the electrolyte will produce scale formation, according to the reaction as follows [21-23]:

$$Ca^{2+} + HCO_3^- + HO^- \rightarrow CaCO_3(s) + H_2O \quad (8)$$

Results obtained by the potentiodynamic polarization of mild steel in free solution (Figure **2**) show that the cathodic current density plateau where its value is ca. - 0.75 µA cm^{-2} corresponding to the limited current by the diffusion of dissolved oxygen. Besides, it can be observed that with the addition of TSC, the cathodic branches shift towards bigger current densities plate. This can be explained by the change of molecule inhibitor orientation at the surface metal [24]. In addition, other authors explained the increase of current density with inhibitor addition, when they used an excess of MTI for bronze corrosion in in 2 g L^{-1} Na_2SO_4 + 2 g L^{-1} $NaHCO_3$ (at pH 5) and they attributed it to the possibilities of side-effect which is the reduction of MTI molecules rather than its desorption from the bronze surface since the anodic current densities remain essentially unchanged [25]. In contrast, for the anodic branches, no limiting current plate was detected. Further, it is seen that that the anodic current density (i_{corr}) significantly decreases with TSC addition as well as shifting the corrosion potential (E_{corr}) towards more anodic potential. This finding suggests that TSC product acts only on the anodic sites and classifies as an anodic-type inhibitor. This can be explained by the specific adsorption of TSC anions onto mild steel to prevent the dissolution process by blocking the active sites on its surface. Thus, the adsorption of TSC anions on the metallic surface is in competition with the Cl^- and SO_4^{2-} ions presented in the solution (see below, PZC study) which led to decreasing the chloride and sulfide ions attack on the surface [11].

However, Table **3** indicated that the addition of TSC has a beneficial effect even at low concentrations, where its inhibition efficiency increases with the

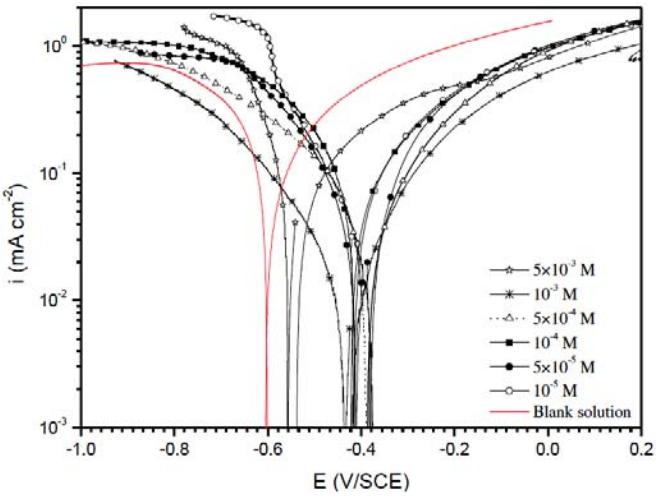

Figure 2: Potentiodynamic polarization curves obtained for mild steel in synthetic cooling water at various concentrations of TSC (*T* = 305 K; *Ω* = 1000 rpm).

Table 3: Electrochemical Parameters for Mild Steel in Synthetic Cooling Water without and with Addition of TSC at Various Concentrations (*T* = 305 K; *Ω* = 1000 rpm).

	Conc. (M)	E_{corr} (mV/SCE)	i_{corr} (µA cm^{-2})	b_a (mV dec^{-1})	η_{PP} (%)
Blank solution	00	-605	102.00	305	-
TSC	10^{-5}	-395	49.14	241	51.8
	5×10^{-5}	-378	39.12	214	61.6
	10^{-4}	-412	20.71	212	79.7
	5×10^{-4}	-385	14.15	197	86.1
	10^{-3}	-420	8.78	178	91.4
	5×10^{-3}	-548	13.05	291	87.2

inhibitor addition, to attain a maximum of 91.4 % at 10^{-3} M of TSC. After this optimum concentration, an gradually decreases of inhibition (a.c. 87.2 %) was observed, which can be attributed to the formation of soluble TSC-Fe and/or TSC-Ca complexes [11, 26].

However, the inhibition efficiencies evaluated by potentiodynamic polarization method were compared with those obtained by electrochemical impedance spectroscopy. In this method, the electrode surface state is not changed by the potential perturbation, and it can be used to monitor the inhibition evolution with time for mild steel, as will be shown below. In contrast, in the case of potentiodynamic polarization measurement where since high anodic polarization may modify markedly the electrode surface state.

Figure **3** shows the Nyquist plots of mild steel in synthetic cooling water without and with different concentration of TSC after 1 h of immersion time at the open circuit potential (E_{OCP}). In these diagrams, two not clearly separated loops were observed. The first can be attributed to the layer of the formed products and the second can be related to the charge transfer resistance in parallel with the double layer capacitance. The proposed electrical equivalent circuit used for fitting experimental diagrams is presented Figure **4**. Thus, the used circuit was composed by R_s , R_{ct} R_{ad}, and R_p whose represent the resistance of electrolyte, the charge transfer, the formed product layer, and the polarization (R_p= R_{ct} + R_{ad}), respectively. It also contains the Q_{ad} and Q_{dl} which are the constant phase elements used to replace the formed product layer and the double layer capacitances, respectively. The use of constant phase elements links to the deviations caused by the surface roughness [27, 28]. Thus, the impedance of CPE was given as follows:

$$Z_{CPE} = Q^{-1}\left(j\omega\right)^{-n} \quad (9)$$

where *Q*, *ω, j* and *n* are the constant phase element (*CPE*), the sine wave modulation angular frequency,

the imaginary number and the *CPE* exponent, respectively. According to *n* value, the CPE can be resistance [Z_{CPE} = *R*, *n* = 0], pure capacity [Z_{CPE} = *C*, *n* = 1], inductance [Z_{CPE} = *L*, *n* = -1] or Warburg impedance (*n* = 0.5) [29]. In addition, the effective calculated double layer capacitance (*C*) derived from the *CPE* parameters as follows [30]:

$$C = Q^{\frac{1}{n}} \times R^{\frac{(1-n)}{n}} \quad (10)$$

The non-linear regression calculation to extract the equivalent circuit elements value by Z-View program was made for each TCS concentration. It can be observed that the experimental and calculated data superimposes almost perfectly (Figure **3**), indicating the validity of the proposed equivalent circuit. On the other hand, it is noticed that the impedance diagrams are significantly changed with the TSC addition, as can be seen in Figure **3**, suggesting a change in the corrosion process of the mild steel/electrolyte interface.

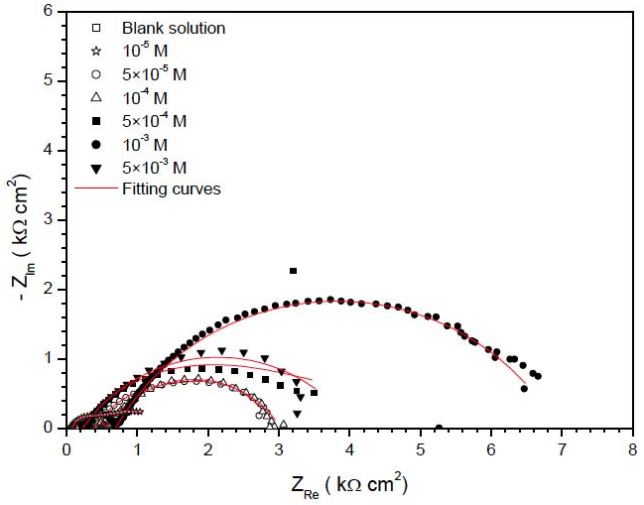

Figure 3: Nyquist plots for mild steel in synthetic cooling water at E_{OCP} containing different concentrations of TSC (Scatter : experimental curves – Red lines: fitting curves) (*T* = 305 K; *Ω* = 1000 rpm).

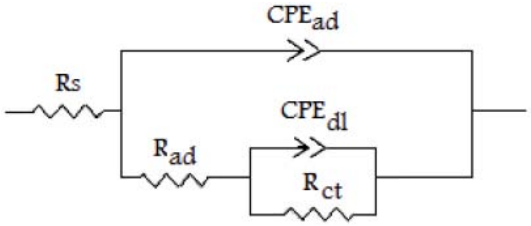

Figure 4: Proposed electrical equivalent circuit for fitting the impedance spectra.

The evolution of the impedance parameters derived from the Nyquist plots and the calculated polarization resistance R_p and inhibition efficiency is presented graphically in Figure **5a-d**. It can be seen that the adsorbed layer resistance R_{ad} and the charge transfer resistance R_{ct} values increase (Figure **5b**) with TSC concentration while the C_{ad} and C_{dl} capacities (Figure **5a**) decrease. These can be explained by the increase of blocking electrode surface portion due to the TSC molecules adsorption [31] and/or by the increase of the homogeneity of the electrode surface. At the same, it is noticed that the n_{ad} and n_{dl} values increase (Figure **5c**) with TSC concentration, confirming also the homogeneity of mild steel surface which is the result of the adsorption of TSC molecules on the metallic surface [32].

However, it is seen that that the polarization resistance R_p and inhibition efficiency values increase (Figure **5d**) with TSC concentration reaching a maximum value at 10^{-3} M of TSC. These results correlate and confirm those obtained from potentiodynamic polarization curves.

3.2. Effect of Immersion Time

However, in order to evaluate the performance of TSC with time, the electrochemical impedance spectroscopy for mild steel in synthetic cooling water with 10^{-3} M of TSC at different immersion time, was carried out at E_{OCP}. The variation extracted electrochemical parameters and the calculated polarization resistance R_p and inhibition efficiency values are offered graphically in Figure **6a-d**. It can be noticed that the adsorbed layer resistance R_{ad} and the charge transfer resistance R_{ct} values rise (Figure **6b**) with time. This finding can be explained by the formation of a stable protective layer on mild steel surface strengthening with immersion time. Furthermore, it is remarked that the C_{ad} and C_{dl} values (Figure **6a**) decrease with immersion time. The decrease in C_{dl} value with immersion time can be explained by a smaller area of mild steel in contact with corrosive solution beneath the corrosion product layer or a less conductivity of the formed film [33]. The R_{ad} and C_{ad} changes measure also the stability of the formed layer on the mild steel surface. On the other hand, the same evolution was attributed to gradual replacement of water molecule by the chloride anions and/or the adsorption of inhibitor molecules on the metal surface, diminishing the dissolution reaction extent [11].

At the same, it is noticed that the n_{ad} and n_{dl} values increase (Figure **5c**) with immersion time, confirming

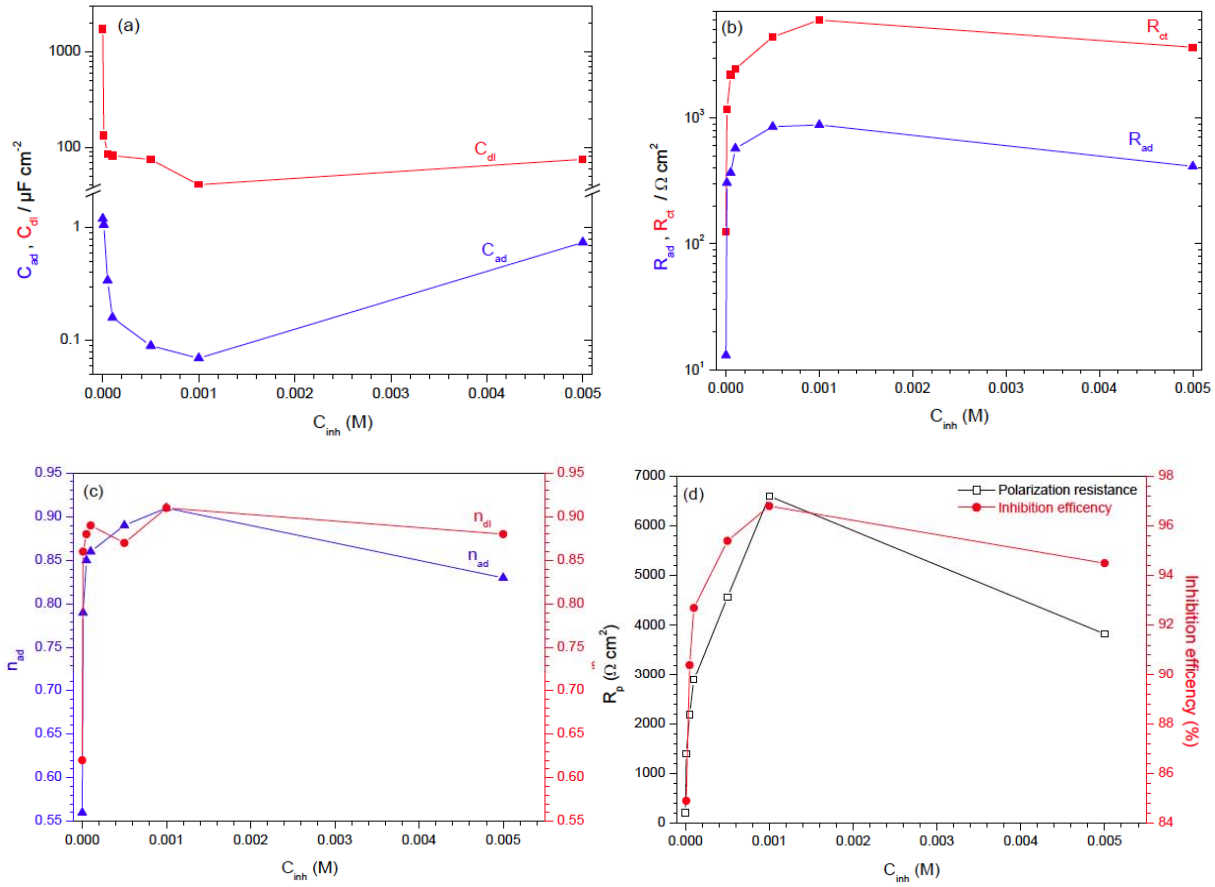

Figure 5: Extracted EIS parameters for mild steel in synthetic cooling water without and with addition of different TSC concentrations.

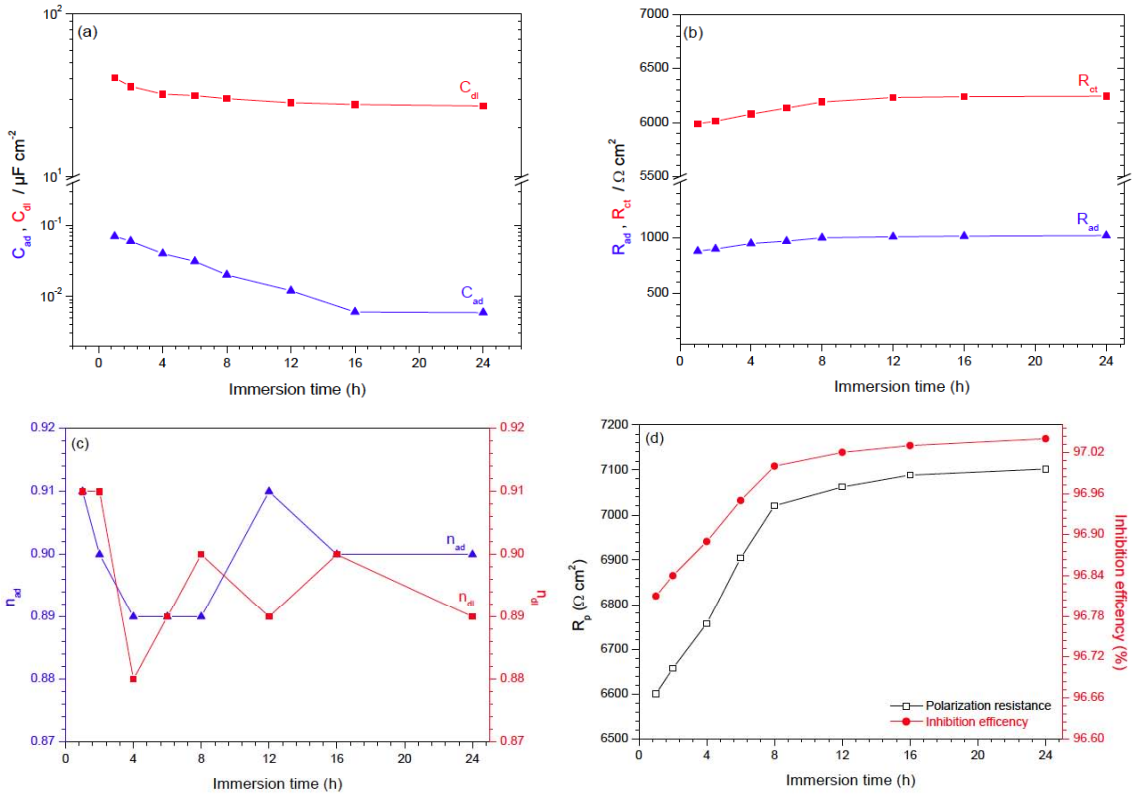

Figure 6: Extracted EIS parameters for mild steel in synthetic cooling water with 10^{-3} M of TSC at difference immersion time.

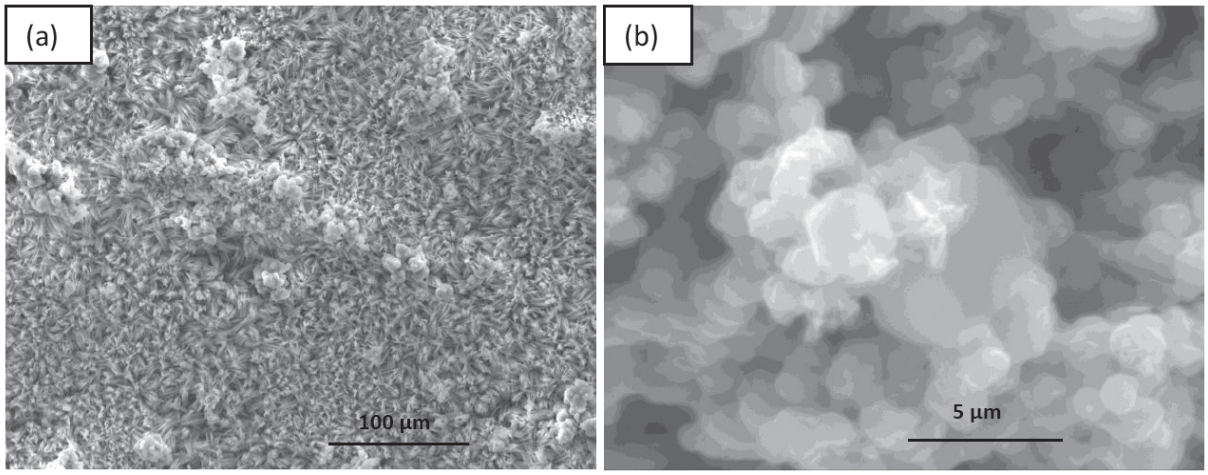

Figure 7: SEM micrographs of mild steel surface after 15 days immersion in blank solution at E_{OCP} (T = 305 K; Ω = 0 rpm).

also the homogeneity of mild steel surface, as mentioned above, by the formation protective layer on the metal surface which became stable, thicker and less permeable with time.

Consequently, it is seen that that the polarization resistance R_p and inhibition efficiency values remain stable over time increase (Figure **6d**) indicating that the TSC take its performance with time and makes it a suitable alternative as an environmentally friendly corrosion inhibitor in cooling water system.

3.3. Surface Analysis, Adsorption Isotherm and Proposed Mechanism

Figure **7a-b** presents the morphology of mild steel surface after 15 days of immersion in synthetic cooling water solution in the absence of TSC (blank solution). It can be seen the subtract surface was greatly damaged, as the corrosion products show a multi-layer morphology (spongy layer). The outer layer of the corrosion products appears uneven and rough, which is compactly adsorbed to the inner layer. Furthermore, Figure **7b** shows sharp and pointed crystal structures indicating the formation of a heterogeneous layer of scale products. However, in our previous works, the EDAX analysis further confirmed the formation of corrosion and scale products by identification of their characteristic elements [34]. In contrast, the morphology of mild steel surface after 15 days of immersion in synthetic cooling water solution in the presence of 10^{-3} M of TSC (Figure **8**), reveals almost no corrosion and scale products and the grooves due to the initial surface abrasion remain clearly visible after 15 days of immersion. This finding can be explained by the formation of a protective layer on mild steel surface. Therefore, the comparison of these two figures reveals a marked inhibition efficiency of TSC and it is in good agreement with the obtained results of electrochemical measurements.

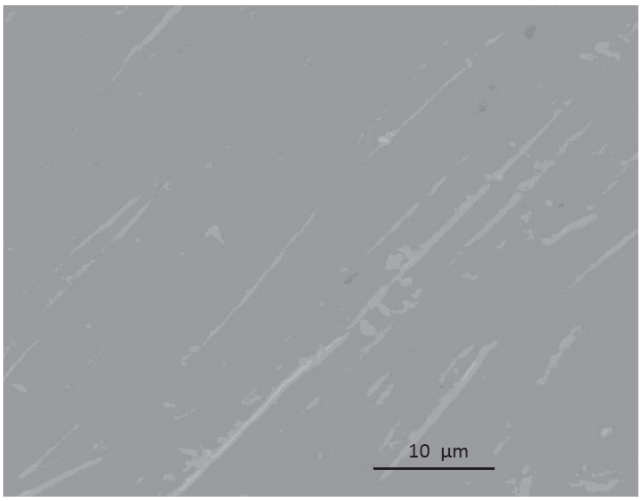

Figure 8: SEM micrographs of mild steel surface after 15 days immersion in blank solution in the presence of 10^{-3} M of TSC at E_{OCP} (T = 305 K; Ω = 0 rpm).

On the other hand, in order to know the adsorption nature of TSC on mild steel, several adsorption isotherms were tested. In fact, Tempkin, Langmuir, Frumkin, Freundlich and Flory–Huggins isotherms, were used to assess the adsorption behavior of TSC [35]. So, the coverage surface (θ) was determined from AC impedance using the above equation (6) (where θ = η/100). In this study, the tested adsorption isotherms and their calculated parameters are illustrated in Table **4**. It is found that the plot of C_{inh}/θ versus C_{inh} shows a straight line (R^2 = 0.9999, slope = 1.03) indicating that adsorption follows the Langmuir adsorption isotherm as shown in Figure **9**. According to this finding, it can be mentioned that TSC forms a mono-layer on the mild

steel surface at the maximum inhibitor concentration, no interaction between the adsorbed species on mild steel surface, and TSC is adsorbed on the mild steel surface as follows : Fe| + TSC → Fe--TSC

In addition, the equilibrium constant of adsorption process (K_{ads}) may be determined according to the above agreements [11], and it is linked to the free energy of adsorption (ΔG^*_{ads}) as follows [36]:

$$K_{ads} = \frac{1}{55.55}\exp(-\frac{\Delta G^*_{ads}}{RT}) \quad (11)$$

where 55.55, *R* and *T* represent the water concentration in solution (mol L^{-1}), the universal gas constant, and the absolute temperature, respectively.

Then, the obtained value of K_{ads} is about 2.46×10^7 L mol^{-1}. This high value reflects the high adsorption ability of TSC on mild steel surface, while the negative value of ΔG^*_{ads} (-41.75 kJ mol^{-1}) reveals the spontaneity of adsorption process and the stability of the formed layer on the mild steel surface [37]. Furthermore, according to the obtained value of ΔG^*_{ads} , it is decided that, the adsorption of TSC molecules on mild steel surface is a mixed type of chemical and physical adsorptions with predominantly the first one [38- 40].

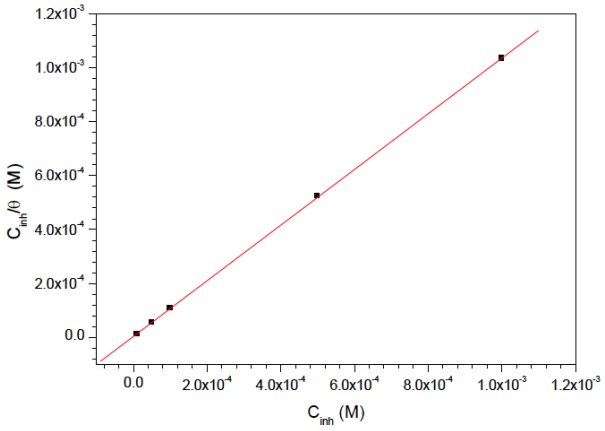

Figure 9: Langmuir isotherm adsorption model of TSC on the mild steel surface in synthetic cooling water (Ω = 1000 rpm).

It is generally assumed that the proceeding of physical adsorption requires the presence of both electrically charged surface of the metal, charged species in the electrolyte and the ionic form of inhibitor. As the different interactions require specific orientations, with the exception of the electrostatic one, it is indefinable to consider steric circumstances with in the molecules that may favour certain interactions and make other less likely or utterly impossible [41]. So, the chemisorption process includes the share or transfer of charge from the molecules to the metallic surface to form a coordinate type bond, which is a possible in case of a positive or a negative charge of the surface [42]. So, this process is influenced on the metal surface charge, on the charge (or on the dipole moment) of inhibitor molecule and on the adsorption of the other ionic species present in the electrolyte [43]. The surface charge can be defined by the position of the corrosion potential E_{corr} with respect to the respective potential of zero charge (PZC). According to the difference value $\varphi = E_{corr} - E_{PZC}$, where φ is the Antropov's "rational" corrosion potential [42]. In our previous work, it is found by electrochemical impedance spectroscopy that the mild steel surface was positively charged such as mentioned in Ref. [31]. It is found that the figure represents a minimum at – 650 mV/SCE, which is more negative than the corrosion potential (- 605 mV/SCE) indicating that the potential φ is positive (($\varphi = E_{corr} - E_{q=0}$= -605 - (-650) = 45 mV/SCE).

Different type of adsorption can be considered for TSC molecules based on mild steel PZC. In synthetic cooling water solution the following mechanism is proposed for the corrosion of mild steel without and with TSC. So, in the absence of TSC the reaction follows the way:

$$Fe + Cl^- - (FeCl^-)_{ads} \quad (12)$$

$$Fe + SO_4^{2-} - (FeSO_4^{2-})_{ads} \quad (13)$$

So, when mild steel immersed in the synthetic cooling water solution, in the presence of TSC, chloride and sulfide ions are firstly adsorbed onto mild steel surface, because of smaller degree of hydration. Adsorbed chloride and sulfide ions create an excess negative charge towards the solution (equations 12 and 13), and favour more adsorption of the tri-sodium citrate salt (Na^+, TSC noted Inh^+) via Cl^- and SO_4^{2-} ions which forms interconnecting bridges between the metal atoms and the organic salt (equations 14 and 15) as proposed follows :

$$(FeCl^-)_{ads} + Inh^+ - (FeCl^-Inh^+)_{ads} \quad (14)$$

$$(FeSO_4^{2-})_{ads} + Inh^+ - (FeSO_4^{2-}Inh^+)_{ads} \quad (15)$$

Therefore, TSC interferes with the reaction of dissolution by metal surface adsorption in two different ways. In the first step, the positively charged metal surface was becoming negative, by chloride and sulfide

Table 4: Curve Fitting Results of TSC Adsorption for Different Adsorption Isotherms

Isotherms	Linear forms	Curves	Parameters	Fitting values
Langmuir	$\frac{C_{inh}}{\theta} = \frac{1}{K_{ads}} + C_{inh}$	$\frac{C_{inh}}{\theta} = f(C_{inh})$	R^2	0.99998
			K_{ads} (L mol^{-1})	2.55×10^{5}
			Slope	1.03107
Freundlich	$\ln(\theta) = \ln(K_{ads}) + \frac{1}{n}\ln(C_{inh})$	$\ln(\theta) = f(\ln(C_{inh}))$	R^2	0.98135
			K_{ads} (L mol^{-1})	1.1787
			Slope (1/n)	0.0275
			n	36.36
Temkin	$\theta = \frac{1}{f}\ln(K_{ads}) + \frac{1}{f}\ln(C_{inh})$	$\theta = f(\ln(C_{inh}))$	R^2	0.98472
			K_{ads} (L mol^{-1})	7.96×10^{19}
			Slope (1/f)	0.02502
			f	39.96
Frumkin	$\ln(C_{inh}\times\frac{1-\theta}{\theta}) = -\ln(K_{ads}) - 2f\theta$	$\ln(C_{inh}\times\frac{1-\theta}{\theta}) = f(\theta)$	R^2	0.98553
			K_{ads} (L mol^{-1})	1.06×10^{15}
			Slope (-2f)	24.95287
			f	-12.47643
Flory-huggins	$\ln(\frac{\theta}{C_{inh}}) = \ln(K_{ads}) + a\ln(1-\theta)$	$\ln(\frac{\theta}{C_{inh}}) = \ln(1-\theta)$	R^2	0.99561
			K_{ads} (L mol^{-1})	1.91×10^{7}
			Slope (a)	2.92257

where f is the factor of energetic inhomogeneity and the parameter ˝ a˜ is the water molecules number replaced by inhibitor molecules on metallic surface, respectively.

ions adsorption as explained above. So, the negatively charged TSC anion will replace with Cl^- and SO_4^{2-} ions adsorbed on the anodic sites, due to more capability of interaction of TSC (having $3O^-$ in its structure) than Cl^- and SO_4^{2-} ions, resulting with exchange of these two ions (competitive) and/or forming $(FeCl^-Inh^+)_{ads}$ (cooperative) as indicated above.

4. CONCLUSION

- Potentiodynamic polarization curve and electrochemical impedance spectroscopy indicated that the addition of TSC compound to synthetic cooling water solution reduces corrosion of mild steel.
- It is found that TSC acts as an anodic–type inhibitor for mild steel in synthetic cooling water solution and its inhibition efficiency values increase with its concentration and reaches a maximum at 10^{-3} M.
- EIS measurements indicated that the inhibition efficiency of TSC improves with immersion time until 24 h.
- The SEM observations showed that the tested inhibitor keeps also its efficiency after 15 days of immersion.
- The adsorption of TSC molecules on the mild steel in synthetic cooling water medium obey Langmuir adsorption isotherm with a formation of a protective monolayer film
- The values of K_{ads} and ΔG^*_{ads} indicate that spontaneous interaction with surface and high adsorption ability of TSC.
- According to PZC values, the different inhibition mechanism was proposed for TSC (competitive and/or cooperative action).
- The good inhibition efficiencies of TSC in synthetic solution makes it a suitable alternative as environmentally friendly corrosion inhibitor in deicing solutions in which tri-sodium citrate is a main component.

REFERENCES

[1] Sherif El-Sayed M. Effects of 5-(3-aminophenyl)-tetrazole on the inhibition of unalloyed iron corrosion in aerated 3.5%

sodium chloride solutions as a corrosion inhibitor. Mater Chem Phys 2011; 129(3): 961-967. https://doi.org/10.1016/j.matchemphys.2011.05.043

[2] Zhang S, Tao Z, Li W, Hou B. The effect of some triazole derivatives as inhibitors for the corrosion of mild steel in 1 M hydrochloric acid. Appl Surf Sci 2009; 255(15): 6757-63. https://doi.org/10.1016/j.apsusc.2008.09.089

[3] Quraishi MA, Sardar R. Corrosion inhibition of mild steel in acid solutions by some aromatic oxadiazoles. Mater Chem Phys 2003; 78(2): 425-31. https://doi.org/10.1016/S0254-0584(02)00299-7

[4] Sherif EM, El Shamy AM, Ramla MM, El-Nazhawy AOH. 5-(Phenyl)-4H-1,2,4-triazole-3-thiol as a corrosion inhibitor for copper in 3.5% NaCl solutions. Mater Chem Phys 2007; 102(2-3): 231-39. https://doi.org/10.1016/j.matchemphys.2006.12.009

[5] Sherif EM, Park SM. Inhibition of Copper Corrosion in 3.0% NaCl Solution by N-Phenyl-1,4-phenylenediamine. J Electrochem Soc 2005; 152(10): B205. https://doi.org/10.1149/1.2018254

[6] Sherif EM, Park SM. Effects of 1,4-naphthoquinone on aluminum corrosion in 0.50 M sodium chloride solutions. Electrochim Acta 2006; 51(7): 1313-21. https://doi.org/10.1016/j.electacta.2005.06.018

[7] Stupnisek-Lisac E, Podbrscek S, Soric T. Non-toxic organic zinc corrosion inhibitors in hydrochloric acid. J Appl Electrochem 1994; 24(8): 779-84. https://doi.org/10.1007/BF00578094

[8] Ramesh S, Rajeswari S, Maruthamuthu S. Effect of inhibitors and biocide on corrosion control of mild steel in natural aqueous environment. Mater Lett 2003; 57(29): 4547-54. https://doi.org/10.1016/S0167-577X(03)00360-4

[9] Riggs OL Jr., Corrosion Inhibitors, 2nd ed., Nathan C.C., Houston, TX, 1973.

[10] Lake DL. Approching environmental acceptability in cooling water corrosion inhibitor. Corrosion Prevention and Control 1988; p. 113.

[11] Touir R, Cenoui M, El Bakri M, Ebn Touhami M. Sodium Gluconate as Corrosion and Scale Inhibitor of Ordinary Steel in Simulated Cooling Water. Corros Sci 2008; 50(6): 1530-37. https://doi.org/10.1016/j.corsci.2008.02.011

[12] Touir R, El Bakri M, Dkhireche N, Ebn Touhami M, Rochdi A. Operational parameters effect of sodium gluconate inhibition used in the protection of cooling water system. J Mater Env Sci 2010; 1(S1) 317-28. https://doi.org/10.1016/j.desal.2009.06.068

[13] Touir R, Dkhireche N, Ebn Touhami M, Lakhrissi M, Lakhrissi B, Sfaira M. Corrosion and scale processes and their inhibition in simulated cooling water systems by monosaccharides derivatives, Part I: EIS study. Desalination 2009; (249): 922-28.

[14] Farr JPG, Saremi M. Molybdate in aqueous corrosion inhibition part II: Effects of molybdate, citrate and phosphate on the anodic behaviour of steel. Surf Technol 1982; 17: 19-27. https://doi.org/10.1016/0376-4583(82)90057-7

[15] Maliekkal BP, Kakkassery JT, Palayoor VR. Efficacies of sodium nitrite and sodium citrate-zinc acetate mixture to inhibit steel rebar corrosion in simulated concrete interstitial solution contaminated with NaCl. Int J Ind Chem 2018; 9(2): 105-14. https://doi.org/10.1007/s40090-018-0142-7

[16] Touir R, Dkhireche N, Ebn Touhami M, Sfaira M, Senhaji O, Robin JJ, Boutevin B, Cherkaoui M. Study of phosphonate addition and hydrodynamic conditions on ordinary steel corrosion inhibition in simulated cooling water. Mater Chem Phys 2010; (122): 1-9. https://doi.org/10.1016/j.matchemphys.2010.02.063

[17] Dkhireche N, Abdelhadi R, Ebn Touhami M, Oudda H, Touir R, Elbakri M, Saira M, Hammouti B, Senhaji O, Taouil R. Elucidation of Dimethyldodecylphosphonate and CTAB Synergism on Corrosion and Scale Inhibition of Mild Steel in Simulated Cooling Water System. Int J Elect Sci 2012; (7): 5314 - 30

[18] Zheng J, Li YQ. One-pot synthesis of tetrahydrobenzo[b] pyran and dihydropyrano [c] chromene derivatives in aqueous media by using trisodium citrate as a green catalyst. Arch App Sci Res 2011; 3(2): 381-88.

[19] Purna SKG, Pollard A, Metzger LE. Effect of Formulation and Manufacturing Parameters on Process Cheese Food Functionality - I. Trisodium Citrate. J Dairy Sci 2006; 89(7): 2386-96. https://doi.org/10.3168/jds.S0022-0302(06)72311-6

[20] Tolwani AJ, Campbell RC, Schenk MB, Allon M. Warnock DG. Simplified citrate anticoagulation for continuous renal replacement therapy. Kidney Inter 2001; 60(1): 370-74. https://doi.org/10.1046/j.1523-1755.2001.00809.x

[21] Chen Y, Hong T, Gopal M, Jepson WP. EIS studies of a corrosion inhibitor behavior under multiphase flow conditions. Corros Sci 2000; 42: 979-90. https://doi.org/10.1016/S0010-938X(99)00127-4

[22] Marín-Cruz J, Cabrera-Sierra R, Pech-Canul MA, González I. EIS study on corrosion and scale processes and their inhibition in cooling system media. Electrochim Acta 2006; 51: 1847-54. https://doi.org/10.1016/j.electacta.2005.02.104

[23] Cachet C, Wiart R. Zinc Electrowinning in Acidic Sulfate Electrolytes: Impedance Analysis and Modeling of the Influence on Nickel Impurities. J Electr Soc 1994; 141: 131-40. https://doi.org/10.1149/1.2054672

[24] Cenoui M, Dkhireche N, Kassou O, Ebn Touhami M, Touir R, Dermaj A, Hajjaji N. Synergistic influence of molybdate ions with TDMTAA on corrosion inhibition of ordinary steel in cooling water system. J Mater Environ Sci 2010; 1(2): 84-95.

[25] Marusic K, Curkovic HO, Takenouti H. Inhibiting effect of 4-methyl-1-p-tolylimidazole to the corrosion of bronze patinated in sulphate medium. Electrochim Acta 2011; 56(22): 7491-7502. https://doi.org/10.1016/j.electacta.2011.06.107

[26] Mansfeld F. Corrosion Mechanisms, Marcel Dekker, New York, 1987; p. 119.

[27] Felhosi I, Telegdi J, Palinkas G, Kalman E. Kinetics of self-assembled layer formation on iron. Electrochim Acta 2002; 47: 2335-40. https://doi.org/10.1016/S0013-4686(02)00084-1

[28] Georges C, Rocca E, Steinmetz P. Synergistic effect of tolutriazol and sodium carboxylates on zinc corrosion in atmospheric conditions. Electrochim Acta 2008; 53: 4839-45. https://doi.org/10.1016/j.electacta.2008.01.073

[29] Tsuchiya H, Fujimoto S, Chihara O, Shibata T. Semiconductive behavior of passive films formed on pure Cr and Fe-Cr alloys in sulfuric acid solution. Electrochim Acta 2002; 47(27): 4357-66. https://doi.org/10.1016/S0013-4686(02)00508-X

[30] Brug GJ, Eeden Van Den ALG, Sluyters-Rehbach M, Sluyters JH. The analysis of electrode impedances complicated by the presence of a constant phase element. J Electroanal Chem Inter Electr 1984; 176(1-2): 275-95. https://doi.org/10.1016/S0022-0728(84)80324-1

[31] Touir R. Nouvelles formulations pour la protection des circuits de refroidissement. Éditions Universitaires Européennes 2016; ISBN: 978-3-639-54733-7.

[32] Rochdi A, Touir R, El Bakri M, Ebn Touhami M, Bakkali S, Mernari B. Protection of low carbon steel by oxadiazole derivatives and biocide against corrosion in simulated cooling water system. J Environ Chem Eng 2015; 3: 233-42. https://doi.org/10.1016/j.jece.2014.11.020

[33] Rahmouni K, Hajjaji N, Keddam M, Srhiri A, Takenouti H. The inhibiting effect of 3-methyl 1,2,4-triazole 5-thione on corrosion of copper in 3% NaCl in presence of sulphide Electrochim Acta 2007; 52: 7519-28. https://doi.org/10.1016/j.electacta.2006.12.079

[34] Belakhmima RA, Dkhireche N, Touir R, Ebn Touhami M. Development of a multi-component SG with CTAB as corrosion, scale, and microorganism inhibitor for cooling water systems. Mater Chem Phys 2015; 152: 85-94. https://doi.org/10.1016/j.matchemphys.2014.12.018

[35] Bastidas JM, Pinilla P, Cano E, Polo JL, Miguel S. Copper corrosion inhibition by triphenylmethane derivatives in sulphuric acid media. Corros Sci 2003; 45(2): 427- 49. https://doi.org/10.1016/S0010-938X(02)00123-3

[36] Kliškic M, Radoševic J, Gudic S. Pyridine and its derivatives as inhibitors of aluminium corrosion in chloride solution. J Appl Electrochem 1997; 27: 947-52. https://doi.org/10.1023/A:1018405803182

[37] Abdallah M. Rhodanine azosulpha drugs as corrosion inhibitors for corrosion of 304 stainless steel in hydrochloric acid solution. Corros Sci 2002; 44(4): 717-28. https://doi.org/10.1016/S0010-938X(01)00100-7

[38] Li X, Deng S, Fu H. Triazolyl blue tetrazolium bromide as a novel corrosion inhibitor for steel in HCl and H2SO4 solutions. Corros Sci 2011; 53(1): 302-09. https://doi.org/10.1016/j.corsci.2010.09.036

[39] Deng S, Li X, Fu H. Two pyrazine derivatives as inhibitors of the cold rolled steel corrosion in hydrochloric acid solution. Corros Sci 2011; 53(2): 822-28. https://doi.org/10.1016/j.corsci.2010.11.019

[40] Ahamad I, Prasad R, Quraishi MA. Inhibition of mild steel corrosion in acid solution by Pheniramine drug: Experimental and theoretical study. Corros Sci 2010; 52(9): 3033-41. https://doi.org/10.1016/j.corsci.2010.05.022

[41] Hosseini M, Mertens SFL, Ghorbani M, Arshadi MR. Asymmetrical Schiff bases as inhibitors of mild steel corrosion in sulphuric acid media. Mater Chem Phys 2003; 78(3): 800-08. https://doi.org/10.1016/S0254-0584(02)00390-5

[42] Popova A, Sokolova E, Raicheva S, Christov M. AC and DC study of the temperature effect on mild steel corrosion in acid media in the presence of benzimidazole derivatives. Corros Sci 2003; 45(1): 33-58. https://doi.org/10.1016/S0010-938X(02)00072-0

[43] Tebbji K, Hammouti B, Oudda H, Ramdani A, Benkadour M. The inhibitive effect of bipyrazolic derivatives on the corrosion of steel in hydrochloric acid solution. Appl Surf Sci 2005; 252(5): 1378-85. https://doi.org/10.1016/j.apsusc.2005.02.097

Received on 20-04-2020 Accepted on 06-05-2020 Published on 14-05-2020

https://doi.org/10.29169/1927-5129.2020.16.02